



ATTI  
DELLA  
SOCIETÀ TOSCANA  
DI  
SCIENZE NATURALI

MEMORIE • SERIE A • VOLUME CXXVI • ANNO 2019



Edizioni ETS



## INDICE - CONTENTS

<p>P. FULIGNATI, P. MARIANELLI, A. SBRANA – Quantitative SEM-EDS analysis of reference silicate mineral and glass samples. <i>Analisi quantitative SEM-EDS di campioni di riferimento di vetri e minerali silicatici.</i></p>	<p>pag. 5</p>
<p>G. GALLELLO, J. BERNABEU, A. DIEZ-CASTILLO, P. ESCRIBA, A. PASTOR, M. LEZZERINI, S. CHENERY, M.E. HODSON, D. STUMP – Developing REE parameters for soil and sediment profile analysis to identify Neolithic anthropogenic signatures at Serpis Valley (Spain). <i>Sviluppo di parametri REE per l'analisi del profilo del suolo e dei sedimenti per identificare le firme antropogeniche neolitiche nella valle del Serpis (Spagna).</i></p>	<p>» 13</p>
<p>D. MAURO, C. BIAGIONI, M. PASERO, H. SKOGBY – Crystal-chemistry of sulfates from the Apuan Alps (Tuscany, Italy). III. Mg-rich sulfate assemblages from the Fornovolasco mining complex. <i>Cristallochimica dei solfati delle Alpi Apuane (Toscana, Italia). III. Associazioni a solfati ricchi in Mg dal complesso minerario di Fornovolasco.</i></p>	<p>» 33</p>
<p>P. ORLANDI, M. D'ORAZIO – Cinnabar and other high-density minerals from stream sediments of Monti Pisani (Pisa and Lucca provinces, Tuscany). <i>Cinabro ed altri minerali ad elevata densità negli "stream sediments" dei Monti Pisani (Province di Lucca e Pisa, Toscana).</i></p>	<p>» 45</p>
<p>M. BACCI, S. CORSI, L. LOMBARDI, M. GIUNTI – Gli interventi di ripristino morfologico ed ecologico del sistema dunale del Golfo di Follonica (Toscana, Italia): tecniche utilizzate e risultati del monitoraggio. <i>Morphological and ecological activities to restore the dune system at the Follonica Gulf (Tuscany, Italy): techniques used and monitoring results.</i></p>	<p>» 57</p>
<p>D. MAGALDI – Interglacial Pleistocene paleosols supporting old roads in central Tuscany. <i>Paleosuoli del Pleistocene interglaciale a supporto di antiche strade nella Toscana centrale.</i></p>	<p>» 67</p>
<p>V. SPADINI – Pliocene scleractinians from Estepona (Malaga, Spain). <i>Sclerattiniani pliocenici di Estepona (Malaga, Spagna).</i></p>	<p>» 75</p>
<p>R. GIANNECCHINI, M. AMBROSIO, A. DEL SORDO, M.T. FAGIOLI, A. SARTELLI, Y. GALANTI – Hydrogeological numerical modeling of the southeastern portion of the Lucca Plain (Tuscany, Italy), stressed by groundwater exploitation. <i>Modello idrogeologico numerico del settore sud-orientale della Piana di Lucca (Toscana, Italia) caratterizzato da sfruttamento intensivo delle risorse idriche.</i></p>	<p>» 95</p>
<p>W. LANDINI – In memoria di Marco Tongiorgi (1934-2019). <i>In memory of Marco Tongiorgi (1934-2019).</i></p>	<p>» 111</p>
<p>Processi Verbali della Società Toscana di Scienza Naturale residente in Pisa. Anno 2019 - <a href="http://www.stsn.it">http://www.stsn.it</a></p>	<p>» 121</p>



PAOLO ORLANDI <sup>(1)</sup>, MASSIMO D'ORAZIO <sup>(2)</sup>

## CINNABAR AND OTHER HIGH-DENSITY MINERALS FROM STREAM SEDIMENTS OF MONTI PISANI (PISA AND LUCCA PROVINCES, TUSCANY)

**Abstract** - P. ORLANDI, M. D'ORAZIO, *Cinnabar and other high-density minerals from stream sediments of Monti Pisani (Pisa and Lucca provinces, Tuscany)*.

We describe the results of a stream sediments survey carried out in the Monti Pisani area (Pisa and Lucca provinces, Tuscany). The survey was initially aimed at locating the primary source of cinnabar (HgS) frequently found as crystal fragments in many streams of Monti Pisani. The search led to the discovery of a small outcrop of phyllitic rocks characterized by an intense low-temperature hydrothermal alteration (kaolinite-halloysite±illite) and by a diffuse, low-grade cinnabar mineralization. As a by-product of this survey we recovered many different types of high-density (> 3.0 g/cm<sup>3</sup>) minerals. These latter are sourced in the Triassic meta-siliciclastic rocks of the "Verrucano" and "Quarziti di Monte Serra" Fms (e.g., garnets, kyanite, staurolite, sillimanite, tourmaline, zircon, Na-amphibole, etc.) and in the sin- and post-Alpine veins and other mineralizations related to hydrothermal activity of variable nature and age (e.g., cinnabar, pyrite, hematite, sphalerite, tourmaline, etc.). Several grains of native gold larger than 100 µm have been also found. Finally, the recovery of several crystal fragments of SiC is quite intriguing and deserves further more specific analyses in order to ascertain their natural or anthropogenic origin.

**Key words** - stream sediments, Monti Pisani, Tuscany, high-density minerals, cinnabar, gold, SiC

**Riassunto** - P. ORLANDI, M. D'ORAZIO, *Cinabro ed altri minerali ad elevata densità negli "stream sediments" dei Monti Pisani (Province di Lucca e Pisa, Toscana)*.

Vengono riportati i risultati di una indagine condotta sugli *stream sediments* dell'area dei Monti Pisani. Questa indagine è stata inizialmente indirizzata a localizzare la sorgente primaria del cinabro (HgS) frequentemente trovato in frammenti di cristalli nei sedimenti di molti torrenti dei Monti Pisani. La ricerca ha condotto alla scoperta di un piccolo affioramento di rocce filladiche caratterizzate da una intensa alterazione idrotermale di bassa temperatura (caolinite-halloysite±illite) e da una diffusa mineralizzazione, a bassa concentrazione, di cinabro. Un sotto-prodotto di questa ricerca è stato il rinvenimento di cristalli e frammenti di cristalli di molte specie di minerali ad elevata densità (> 3.0 g/cm<sup>3</sup>). Questi minerali provengono sia dalle rocce meta-siliciclastiche triassiche delle formazioni del "Verrucano" e delle "Quarziti di Monte Serra" (es., granati, cianite, staurolite, sillimanite, tourmalina, zircone, Na-anfibolo, etc.), sia dai sistemi di vene e altre mineralizzazioni correlate all'attività idrotermale sin- e post-Orogenesi Alpina (es., cinabro, pirite, ematite, sfalerite, tormalina, etc.). Eccezionalmente, sono state trovate anche alcune particelle di oro nativo di dimensioni > 100 µm. Il rinvenimento di alcuni occasionali frammenti di cristalli di SiC è molto interessante, ma richiede ulteriori e più specifiche analisi per accertare la loro origine naturale o antropica.

**Parole chiave** - stream sediments, Monti Pisani, Toscana, minerali ad alta densità, cinabro, oro, SiC

### INTRODUCTION

The systematic mineralogical and geochemical survey of stream sediments is widely used in prospecting, looking for signs of useful mineralizations. Sands collected in the bed of rivers and streams are investigated for identifying their mineral constituents with the aim of localizing primary and alluvial mineralizations. This kind of survey is especially directed to those minerals characterized by high density, hardness and abrasion resistance. Gold and precious stones prospecting are typical examples of searches that successfully used, and still use, stream sediment analysis (e.g., Aichler *et al.*, 2008 and references therein).

The study presented in this work started with the aim of locating a potential primary cinnabar mineralization in the Monti Pisani area (Lucca and Pisa provinces, Tuscany). This search was motivated by the finding of fragments of cinnabar crystals in the stream sediments of several small water courses, both on the Lucca and Pisa slopes of the mountain. Cinnabar was found within sands from streams flowing onto meta-sedimentary rocks (phyllite, quartzite, meta-conglomerate, meta-breccia, schist) of the Paleozoic basement and the continental Triassic sedimentary succession forming the "Verruca" and "Quarziti del Monte Serra" formations (Rau & Tongiorgi, 1974). The occurrence of cinnabar in the Monti Pisani area was reported for the first time by Antonio D'Achiardi (D'Achiardi, 1872-73). In his work "Mineralogia della Toscana" he wrote: "*Sul Monte delle Fate presso San Giuliano entro la Calcaria marmorea, là ove è fissa in più direzioni, trovasi il Cinabro in nidi entro ad altri minerali, specialmente Spato-calcare ferrifero e Malachita, che incrostano le fessure di quella calcaria*" ("on Monte delle Fate, close to San Giuliano, cinnabar occurs inside marble where it is fractured in several directions. It is found as nests within other minerals, especially siderite and mala-

<sup>(1)</sup> Via di Vaccoli, traversa 1, I-55100 Lucca; Email: paolorlandi.pisa@gmail.com

<sup>(2)</sup> Dipartimento di Scienze della Terra, Università di Pisa, Via Santa Maria 53, I-56126 Pisa; Email: massimo.dorazio@unipi.it

Corresponding author: Massimo D'Orazio

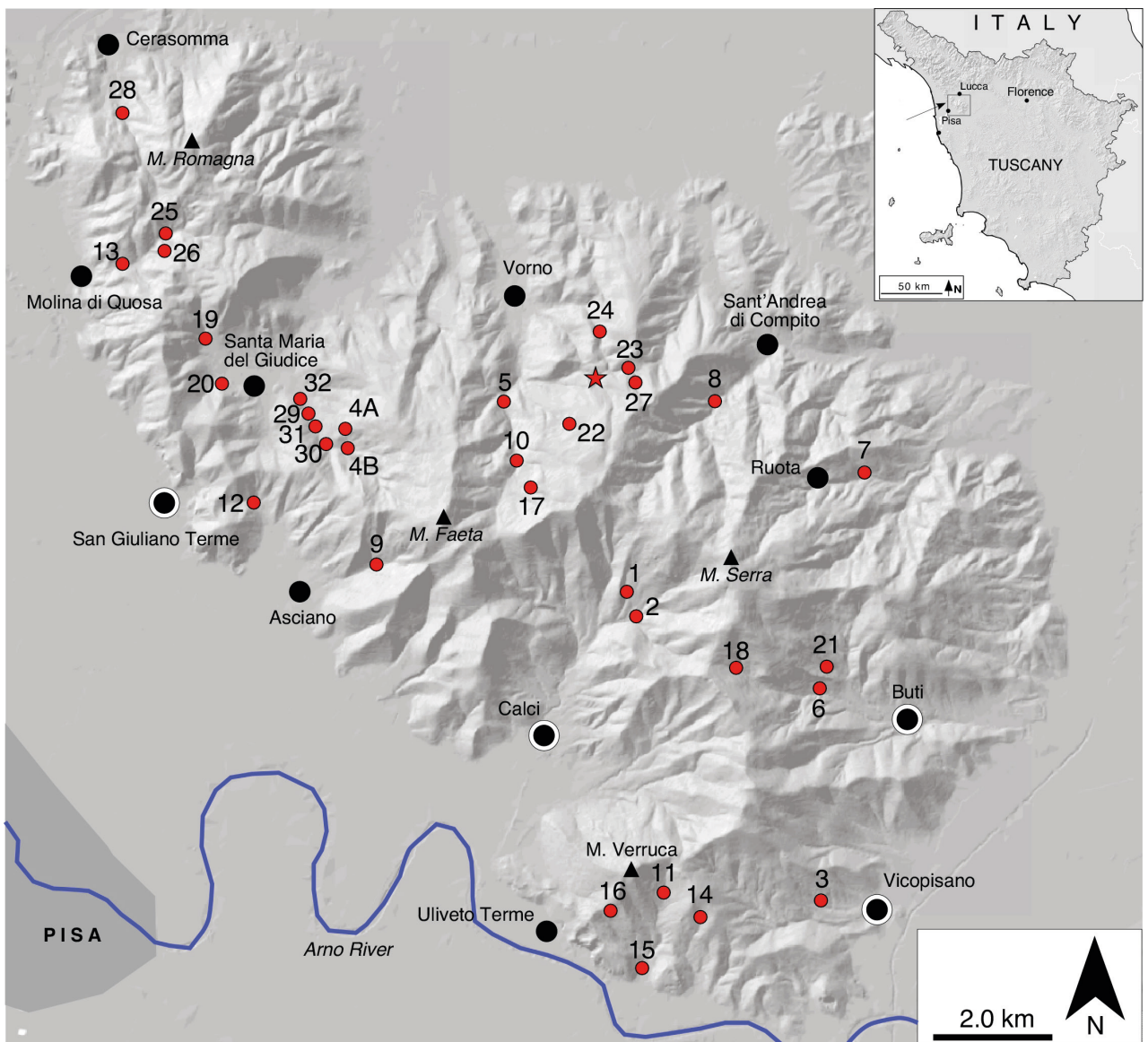


Figure 1. Shaded-relief map of the Monti Pisani showing the sampling sites (red circles), and the municipalities (white-black circles) and villages (black circles) cited in the text. The red star indicates the small area characterized by cinnabar-bearing, low-temperature, hydrothermal rocks.

chite, that encrust the fractures of the marble"). Thus, the localization and mode of occurrence of the primary (here in the sense of not detrital) cinnabar mineralization in the Liassic marble cropping out between the villages of San Giuliano and Asciano was already known since the second half of the XIX century. On the contrary the source of the detrital cinnabar found in the stream sediments of the Monti Pisani was not yet identified.

The Hg anomaly of the marble around San Giuliano was confirmed by a geochemical survey of more than 2000 samples of rocks and stream sediments from the whole Tuscany commissioned by CNEN (Comitato Nazionale per l'Energia Nucleare; Dall'Aglio *et al.*, 1966).

#### SAMPLING AND METHODS

The first sampling of stream sediments was carried out by L. De Fonte during the preparation of his degree thesis (De Fonte, 1996). All the sites studied by De Fonte were sampled again for the present study with the aim of confirming his finding and increase the observations (Fig. 1).

At each sampling site about 100 kg of sediments were collected. They were sieved on site using a metallic grid with 1 cm aperture to discard the coarse fraction. High-density ( $> 3.0 \text{ g/cm}^3$ ) minerals were concentrated using a one meter long riffled sluice placed in the flowing stream water. The sand was repeatedly washed in a

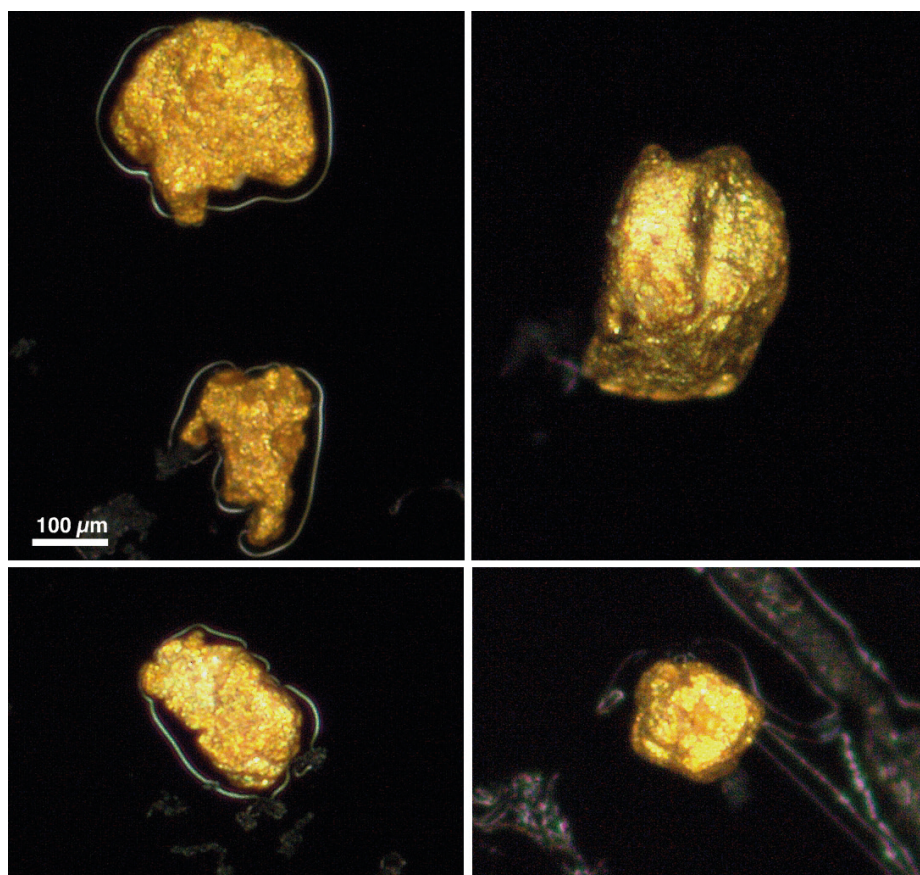


Figure 2. Tiny native gold nuggets from samples #1, #2, #4a. The scale is the same for all the images.

pan in order to increase the concentration of high-density minerals. At the end of this process the residual sand was again sieved, and the fraction  $> 250 \mu\text{m}$  was discarded. Samples were dried and the particles with high magnetic susceptibility were removed first with a strong magnet and successively with a “Frantz” isodynamic magnetic separator. The diamagnetic and low-susceptibility grains were treated with a concentrated solution of sodium polytungstate (density  $2.8 \text{ g/cm}^3$ ) discarding the floating particles.

Mineral identification was thus focused onto high-density, diamagnetic particles. The most common phases were identified observing their macroscopic physical properties under the optical stereo-microscope. Minerals of more uncertain identification were analyzed by X-ray diffraction (114.6 mm Gandolfi camera with Ni-filtered  $\text{CuK}\alpha$  radiation), X-ray fluorescence using X-ray energy-dispersive systems coupled with scanning electron microscope (SEM Philips XL 30 and FEG-SEM FEI Quanta 450), and  $\mu\text{Raman}$  spectroscopy (Jobin-Yvon Horiba XploRA Plus). Analytical data were acquired at the Pisa University’s Dipartimento di Scienze della Terra, except for the FEG-SEM ones that were obtained at the Pisa University’s Centro Interdipartimentale di Scienza ed Ingegneria dei Materiali (CISIM).

Due to the low reproducibility of the sampling and concentration processes carried out in the field, we will not attempt any quantitative estimate of the abundance of the different mineralogical species identified in the sand samples. Indeed the initial quantity of stream sediment sampled was not always the same, and the washing efficiency of the sluice varied largely as a function of the stream flow. Finally, the results of the panning varied from sample to sample. Therefore, the data on the mineralogical composition of the high-density fraction of our samples will be qualitative only.

The sampling sites and the rocks cropping out in the stream drainage basin upstream the sampling sites themselves are reported in Tab. 1. In order to hypothesize the provenance of the minerals identified in each sample, an approximate estimate of the areal proportion of each rock cropping out in the stream drainage basin upstream the sampling site was done using the software ARC/Info on a digitalized version of the 1:25.000 geological map of Monti Pisani (Rau & Tongiorgi, 1974). The results are reported within parentheses in Tab. 1 next to the abbreviations of the geological units. The last column of Tab. 1 lists the high-density minerals found in each sample with a qualitative estimate of their abundance.

Table 1. List of sampling sites, rocks cropping out in the drainage basins upstream the sampling sites, and high-density minerals identified in each sample.

Sample	Locality	Outcropping rocks	Phases identified
1	Botro della Fonte del Porco, Calci	V2 (9%), V3 (<1%), S1 (7%), S2 (1%), S3 (72%), S4 (9%)	Hem (a), Spl (a), Py (b), Lm (a), Rt (d), Ap (d), Zrn (d), Grt (d), Px (e), Tur (d), Ep (e), Cin (d), native mercury (2 small drops), Sn-Hg alloy (1 grain), gold (3 grains), magnetic spherules (d)
2	Botro del Pruno, Calci	V1(15), V2(48), V3(26), S1(5), S2(<1), S3(<1), FpV(5)	Hem (b), Spl (b), Py (c), Lm (b), Ep (d), Ap (d), Zrn (d), Rt (e), gold (2 small grains), magnetic spherules (c)
3	Rio di Romitorio, Vicopisano	V2(38), V3(51), S1(5), S2(2), FpV(4)	Hem (b), Spl (b), Py (b), Lm (a), Rt (d), Ap (d), Zrn (d), Ep (e), magnetic spherules (d), SiC (2 grains)
4a	Rio San Pantaleone, Santa Maria del Giudice	fqB(13), brA(2), V1(4), V2(37), V3(31), S1(10), S2(<1), S3(3)	Hem (a), Spl (b), Py (c), Lm (c), Rt (d), Ap (d), Zrn (d), Grt (d), Tur (d), Mnz (3 grains), magnetic spherules (e), Cin (1 grain), gold (2 grains), SiC (2 grains)
4b	Rio del Rumito, Santa Maria del Giudice	fqB(44), brA(3), V1(8), V2(43), V3(2), S1(<1)	Hem (b), Spl (b), Py (b), Lm (a), Rt (d), Ap (d), Zrn (d), magnetic spherules (e)
5	Rio Vorno, Vorno	V2(4), V3(7), S1(9), S2(6), S3(61), S4(12), FpV(1)	Hem (a), Spl (b), Py (c), Lm (b), Rt (e), Ap (d), Zrn (d), Grt (d), Tur (d), Cin (e), magnetic spherules (d)
6	Rio di Sant'Antone, Buti	fqB(7), V1(3), V2(9), V3(16), S1(22), S2(9), S3(27), S4(6), FpV(1)	Hem (b), Spl (b), Py (a), Lm (a), Rt (d), Ap (d), Zrn (d), Px (e), Tur (d), Cin (e), magnetic spherules (e)
7	Visona di Ruota, Ruota	V2(6), V3(65), S1(17), S2(3), S3(9)	Hem (b), Spl (b), Py (c), Lm (a), Rt (d), Ap (d), Zrn (d), Px (d), Tur (c), magnetic spherules (e)
8	Rio Visona, Sant'Andrea di Compito	V1(2), V2(13), V3(52), S1(16), S2(8), S3(8), S4(1)	Hem (c), Spl (c), Py (c), Lm (a), Rt (d), Ap (d), Tur (c), Cin (e), magnetic spherules (e)
9	Canale di Zambra, Asciano	V3(1), S1(38), S2(9), S3(52)	Hem (a), Spl (b), Py (b), Lm (a), Rt (d), Ap (c), Zrn (d), Grt (d), Tur (c), Cm (1 grain), Mlc (2 grains), magnetic spherules (e)
10	Rio Vorno, Vorno	S1(79), S2(12), S3(9)	Hem (b), Spl (b), Py (c), Lm (a), Rt (d), Zrn (b), Tur (c), Cin (p), magnetic spherules (e)
12	La Valle, Asciano	V3(83), FpV(13)	Hem (a), Spl (b), Py (d), Lm (a), Rt (e), Ap (e), Zrn (c), Grt (e), Px (e), Amp (e), Tur (e), magnetic spherules (e)
13	Fosso dei Mulini, Molina di Quosa	FpV(100)	Hem (a), Spl (a), Py (a), Lm (a), Rt (e), Zrn (e), Grt (c), Tur (c), Cin (b), magnetic spherules (e)
14	Botro della Sassa, Lugnano	V3(36), S1(63), S2(1),	Hem (a), Spl (b), Py (c), Lm (c), Rt (d), Ap (c), Zrn (d), Tur (b), magnetic spherules (e)
15	Rio di Noce, Noce	fqB(5), V1(6), V2(21), V3(16), S1(8), S2(9), S3(19), S4(<1), FpV(16)	Hem (b), Spl (b), Py (c), Lm (a), Ap (c), Zrn (d), Grt (e), Tur (c)
16	Botro dei Lecci, Uliveto Terme	S3(58), S4(1), FpV(41)	Hem (b), Spl (b), Py (a), Lm (b), Rt (e), Ap (d), Zrn (d), Grt (e), Px (e), SiC (2 grains)
17	Rio della Ghiacciaiola, Vorno	S1(44), S2(5), S3(51)	Hem (b), Spl (b), Py (a), Lm (a), Rt (e), Ap (c), Zrn (d), Grt (d), Px (e), Tur (c), magnetic spherules (e)
18	Rio di Sant'Antone, Buti	V2(2), V3(30), S1(35), S2(14), S3(19)	Hem (c), Spl (b), Py (a), Lm (b), Rt (e), Zrn (c), Ep (e), Tur (c)
19	Rio di Bulano, Santa Maria del Giudice	FpV(100)	Hem (b), Spl (a), Py (c), Lm (c), Rt (e), Brk (2 grains), Ap (d), Zrn (d), Grt (e), Px (e), Ep (e), Tur (d), Cin (d)
20	Querceto, Santa Maria del Giudice	FpV(100)	Hem (a), Spl (a), Py (a), Lm (a), Rt (d), Zrn (d), Grt (e), Ep (e), Cm (1 grain)
21	Vallino della Lecceta, Santa Maria del Giudice	fqB(8), V1(17), V2(19), V3(10), S1(19), S2(16), S3(11)	Hem (b), Spl (b), Py (c), Lm (a), Rt (e), Zrn (c), Grt (e), Amp (e), Tur (d), Mnz (3 grains), Brk (2 grains), Cm (1 grain)

22	Fosso di Fossacca, Vormo	V3(45), S1(20), S2(10), S3(25)	Hem (b), Spl (b), Py (c), Lm (a), Rt (d), Ap (c), Zrn (c), Tur (c), Cin (c)
23	Rio di Ciabattaia, Vormo	V2(8), V3(31), S1(4), S3(31), S4(26)	Hem (b), Spl (b), Py (b), Lm (a), Rt (e), Ap (c), Zrn (d), Tur (c), Cin (b).
24	Rio di Ciabattaia, Vormo	V2(10), V3(55), S1(11), S2(5), S3(30), S4(9)	Hem (a), Spl (a), Py (b), Lm (a), Rt (e), Ap (c), Zrn (c), Grt (e), Tur (b), Cin (b)
25	Fosso dei Mulini, Molina di Quosa	FpV(100)	Hem (a), Spl (a), Py (A), Lm (b), Rt (p), Ap (p), Zrn (p), Ep (p), Tur (p), Brk (2 grains), Sp (2 grains)
26	Left tributary of Fosso dei Mulini, Molina di Quosa,	FpV(100)	Hem (b), Spl (b), Py (a), Lm (a), Rt (c), Ap (e), Cin (e)
28	Fosso del Confine, Cerasomma	FpV(100)	Hem (b), Mag (b), Py (a), Lm (a), Rt (e), Grt (e)
29	Rio San Pantaleone, Santa Maria del Giudice	fgB(23), brA(3), V1(8), V2(41), V3(16), S1(4), S2(<1), S3(6)	Hem (a), Spl (a), Py (c), Lm (a), Rt (e), Ap (d), Zrn (d), Grt (e), Ep (e), Amp (e), Px (e), Tur (c), Sil (2 grains), Cin (e), Brk (2 grains), magnetic spherules (d), SiC (1 grain)
30	Rio San Pantaleone, Santa Maria del Giudice	fgB(40), brA(2), V1(9), V2(43), V3(6), S1(<1)	Hem (b), Spl (b), Py (a), Lm (a), Rt (e), Zrn (d), Tur (d), gahnite (1 grain), magnetic spherules (e).
31	Rio San Pantaleone, Santa Maria del Giudice	fgB(24), brA(3), V1(6), V2(40), V3(17), S1(4), S2(<1), S3(6)	Hem (b), Spl (b), Py (a), Lm (a), Rt (c), Ap (c), Zrn (c), Tur (c), magnetic spherules (d)
32	Rio San Pantaleone, Santa Maria del Giudice	fgB(24), brA(3), V1(6), V2(40), V3(17), S1(4), S2(<1), S3(6)	Hem (b), Spl (b), Py (a), Lm (a), Rt (c), Ap (c), Zrn (c), Tur (c), magnetic spherules (d), Grt (b), Ky, Sil, St, Mnz., Cin (e), Px, Mica, Ep, Na-amp, Chl, Omp, Ang (2 grains), Sp (2 grains), Brt (1 grain), Ccp (1 grain)

Note: (a) Extremely abundant; (b) very abundant; (c) abundant; (d) many grains; (e) few grains. Abbreviations of minerals: Amp, amphibole; Ang, anglesite; Ap, apatite; Brk, brookite; Brt, baryte; Ccp, chalcopyrite; Chl, chlorite; Cin, cinnabar; Cm, corundum; Ep, epidote; Na-amp, Na-amphibole; Grt, garnet; Hem, hematite; Ky, kyanite; Lm, limonite; Mlc, malachite; Mnz, monazite; Omp, omphacite; Px, pyroxene; Py, pyrite; Rt, rutile; Sil, sillimanite; Sp, sphalerite; Spl, spinel; St, staurolite; Tur, tourmaline; Zrn, zircon.

Abbreviations of geological units: fgB, "Filladè e quarziti listate di Buti" (phyllite and quartzite, ?Cambrian-?Ordovician); sSL, "Scisti di San Lorenzo" (phyllite, Upper Carboniferous-Lower Permian); brA, "Breccia di Asciano" (meta-breccia and meta-conglomerate, Permian); V1, "Anageniti grossolane" ("Verruca Fm.", meta-conglomerate, Anisic-Ladinic); V2, "Scisti violetti" ("Verruca Fm.", phyllite, Anisic-Ladinic); V3, "Anageniti minute" ("Verruca Fm.", meta-arenite and phyllite, Anisic-Ladinic); S1, "Scisti verdi" ("Quarziti del Monte Serra" Fm., phyllite and quartzite, Carnic); S2, "Quarziti verdi" ("Quarziti del Monte Serra" Fm., quartzite and meta-arenite, Carnic); S3, "Quarziti bianco-rosa" ("Quarziti del Monte Serra" Fm., quartzite and meta-arenite, Carnic); S4, "Quarziti viola zonate" ("Quarziti del Monte Serra" Fm., quartzite and phyllite, Carnic); FpV, metamorphic and non-metamorphic formations younger than the "Quarziti del Monte Serra" Fm.

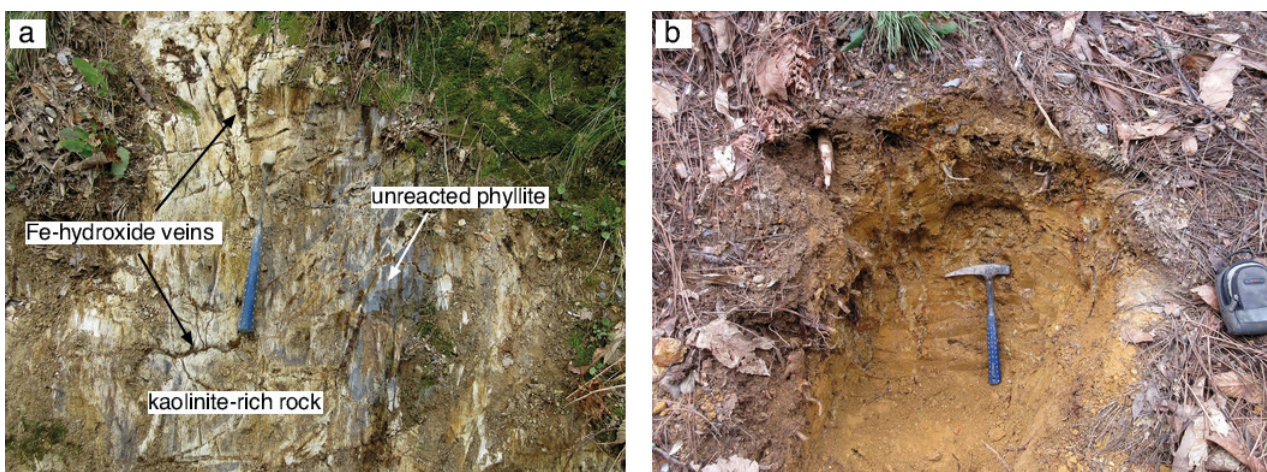


Figure 3. a) The outcrop of kaolinite-rich hydrothermal rock close to Monte Zano (Vorno, Lucca); b) The small trench exposing the cinnabar-bearing clayey material. The hammer is 32.5 cm long.

## RESULTS

The minerals identified in the high-density fraction of the studied samples may be: i) primary clastic components of the pre-Alpine rocks of the Monti Pisani; ii) minerals formed during or after the Alpine Orogeny in relation to hydrothermal activity of variable nature and age. A well-known example of hydrothermal mineralization occurring in the Monti Pisani are the numerous large quartz veins often hosting museum-quality quartz crystals (Dini *et al.*, 1998). As in many cases it is not easy to discriminate the origin of the minerals, in the following we will describe them according to a systematic arrangement, specifying, whenever possible, their most likely provenance.

### Native elements

**Gold:** very tiny gold nuggets were found in samples #1, #2, #4a (Fig. 2). This mineral has been dubitatively associated to the group of detrital minerals even though the grains show features that can be related either to a detrital origin from metasedimentary rocks or to a primary origin in association to Alpine quartz veins. Two very small nuggets, some tens of  $\mu\text{m}$  wide, have a flattened shape showing evident deformations. They could be detrital gold grains from the Paleozoic-Triassic siliciclastic metasedimentary formations of the Monti Pisani. On the other hand, some very small nuggets have a rounded spongy shape lacking clear evidences of a significant abrasion. The provenance of these grains could be very close to the sampling site, possibly inside some of the Alpine quartz veins.

**Mercury:** it was found just as two very small droplets within sample #1. They were found along with several cinnabar grains and a single fragment of Sn-Hg alloy.

### Sulfides

**Chalcopyrite:** it was found as a single, anhedral, golden grain in sample #32.

**Cinnabar:** the casual finding of small cinnabar grains within the sediments of one of the streams flowing in the Monti Pisani area stimulated our search for a new primary Hg mineralization. In the present survey, cinnabar was found in many samples, both on the northern and southern slopes of the mountain. Three samples are particularly enriched in this mineral: #23 and #24 were collected in the bed of Rio Stanghetta, #13 was sampled in the bed of Fosso dei Mulini, close to the hamlet of Molina di Quosa. Cinnabar invariably appears as small, shining and transparent crystal fragments. They have sharp edges and do not show abraded surfaces. We scouted the area around the sampling sites #23, #24 and #13, aiming at finding the traces of a primary cinnabar mineralization. Our search was unsuccessful for the sampling site #13, whereas we found interesting evidences of mineralization in the area of Monte Zano (sampling sites #23 and #24). About 230 m due SW of the Stanghetta locality an unpaved road cuts a small volume of phyllitic rocks which suffered a strong hydrothermal alteration. The original gray-violet phyllite belonging to the "Anageniti minute" member of the Verruca Fm. are here transformed into a whitish, soft rock mainly made of kaolinite/halloysite  $\pm$  illite (Fig. 3a). This rock is crossed by veinlets of iron hydroxides and less abundant quartz veins. This white hydrothermal rock is completely free of cinnabar. About 50 m due S from this road cut we dug three small trenches (about 50 cm deep) in the soil of the wood (Fig. 3b). After the first  $\sim$ 10 cm of organic material-rich horizon, we found about 40 cm of soft, orange-colored clayey material directly overlying the phyllite bedrock from which it is separated by a sharp transition zone. The panning of several samples of this orange clay yielded

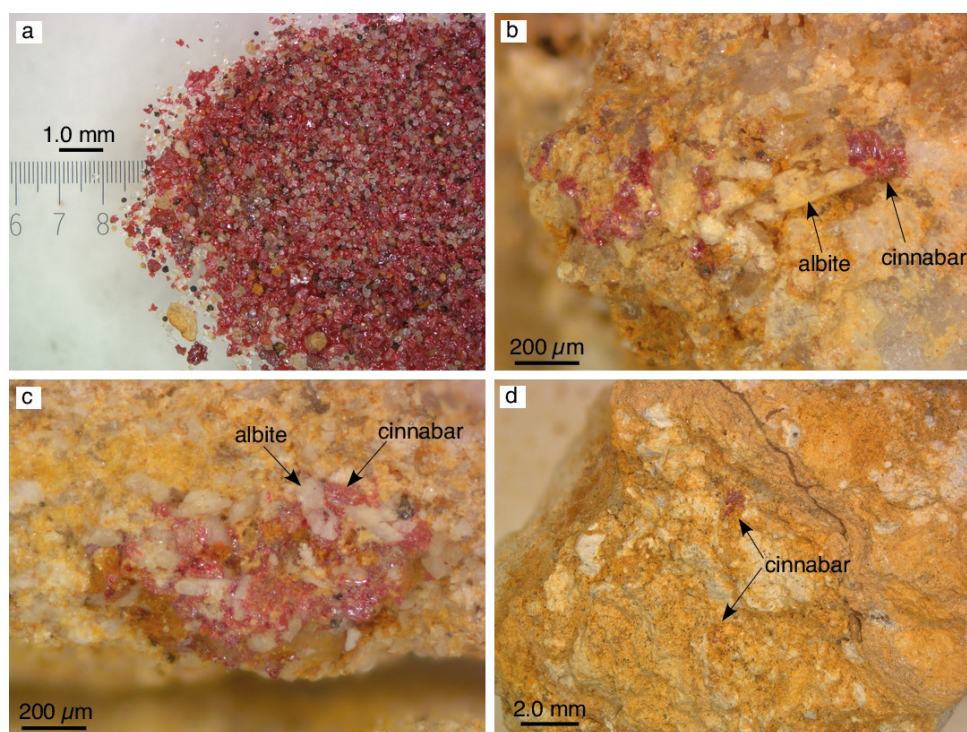


Figure 4. Cinnabar from Monti Pisani. a) cinnabar crystal fragments extracted by panning about ten kilograms of low-temperature hydrothermal material from the small trench in the Monte Zano (Vorno, Lucca) area; b,c,d) crystalline cinnabar *in situ* from the same trench.

abundant cinnabar fragments up to 2 mm in size, and with a maximum concentration of 110 mg/kg (Fig. 4a). Fig. 4b,c,d shows that cinnabar is frequently localized at the interstices of residual albite crystals. Cinnabar is associated with tiny (100-500 µm) euhedral pentagonal dodecahedra of limonitized pyrite. These latter are very common in all the studied samples of stream sediments. *Pyrite*: this mineral is widespread and very abundant in all samples. Crystals showing the typical lustre of the species are rare as most crystals are more or less oxidized into Fe-hydroxides. The most frequent habitus is the pentagonal dodecahedron, less common are cubic crystals and even rarer the octahedral. The sharp edges of the pyrite crystals suggest that this mineral could be a product of Alpine metamorphic or hydrothermal events.

*Sphalerite*: three transparent, yellow or orange-yellow, grains of sphalerite were found in samples #25, #32 (Fig. 5a).

### Oxides and hydroxides

*Brookite*: it was found within samples #19, #25, #29 and identified by SEM-EDS and XRPD. The crystal fragments, translucent and light-brown in color, sometime preserve their pristine tabular habitus.

*Corundum*: this mineral, found just in samples #9, #20, #21, was identified by SEM-EDS and XRPD analyses.

One of the three grains has the optical properties of a gem-quality ruby.

*Gahnite*: just a single grain of this spinel, identified by SEM-EDS and XRPD analyses, was found in the sample #30; it is a colorless vitreous crystal still showing an octahedral shape.

*Goethite*: iron hydroxide (very likely goethite) partially or completely replaces the abundant pyrite crystals found in all the studied samples; this mineral, along with hematite and magnetite, represents the most abundant high-density phase found in the investigated sediments. Goethite also commonly forms as a replacement of siderite.

*Hematite*: this mineral is ubiquitous and abundant in all samples; it occurs as very bright, small, micaceous crystals. The typical primary occurrence of hematite is in Alpine quartz veins in association with siderite and chlorite.

*“Leucoxene”*: with this term we indicate the cream-colored, equant and rounded crystals with a waxy luster constituted by  $\text{TiO}_2$  and commonly found in many samples. The  $\mu\text{Raman}$  spectra of some selected crystals indicate that they are constituted by rutile (Fig. 5b).

*Rutile*: even if this mineral is much harder than apatite, rutile crystals found in the studied stream sediments occur as rounded grains showing dull and abraded

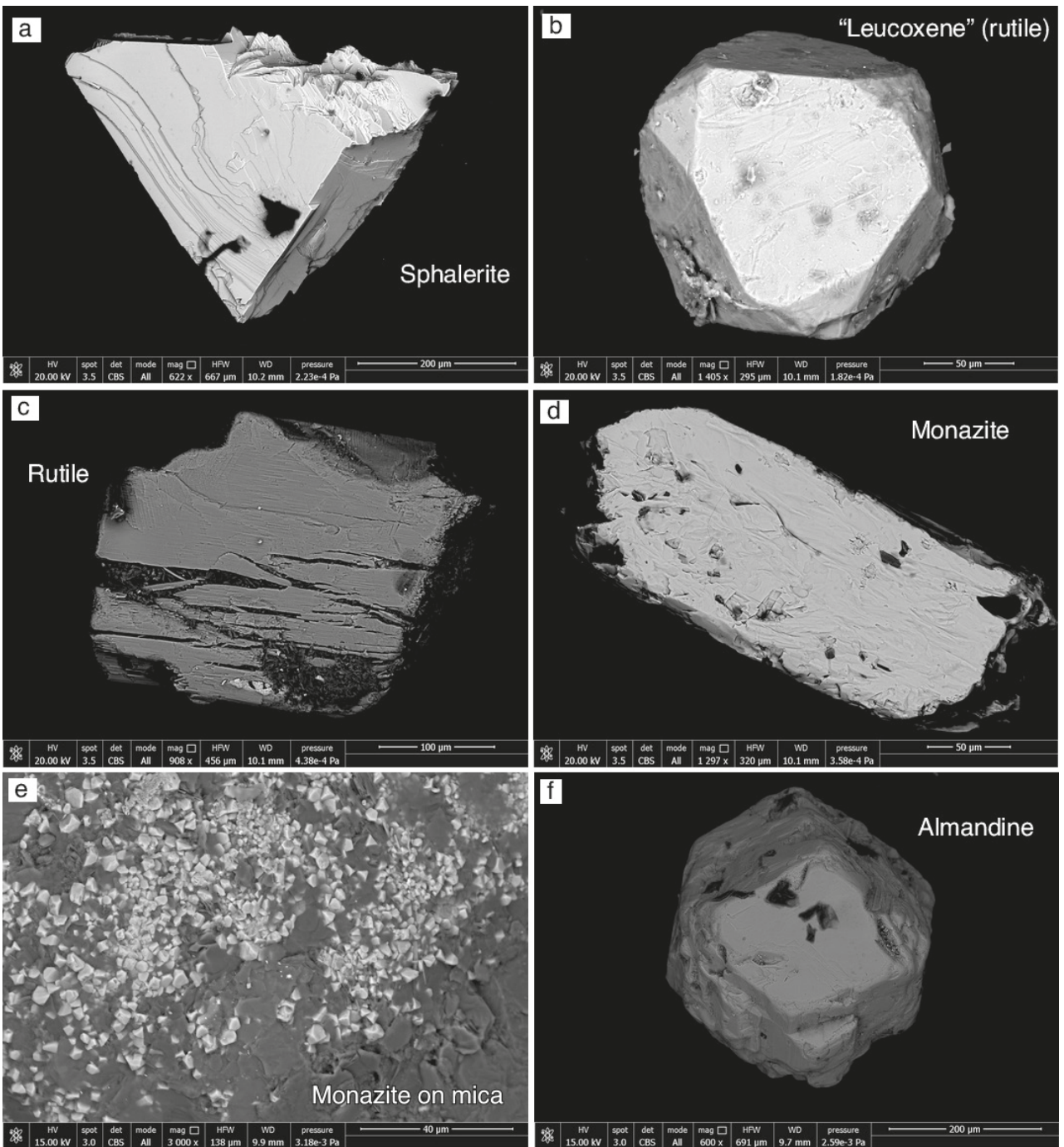


Figure 5. Back-scattered electron images of high-density crystals and crystal fragments extracted from sample #32 (Rio San Pantaleone, Santa Maria del Giudice, Lucca). a) nearly complete tetrahedral crystal of sphalerite; b) equant crystal replaced of "leucoxene"; c) fractured subhedral crystal of rutile; d) subhedral crystal of "monazite"; e) tiny crystals of "monazite" grown on mica; f) euhedral, slightly abraded, dodecahedral crystal of almandine.

surfaces (Fig. 5c). Grains exhibiting crystal faces with a mirror lustre, that would have indicated their occurrence in veins or cracks, were never observed. Generally, rutile grains have a reddish color.

*Spinel (Fe-Ti-Al-Mg)*: crystals and crystal fragments of Fe-Ti-Al-Mg spinel are ubiquitous in the studied samples. They generally occur as black octahedral crystals. The compositions vary from nearly pure magnetite to intermediate between magnetite and *ülvöspinel*, to terms with a significant proportion of pleonaste end-member.

### Sulphates and phosphates

*Anglesite*: two yellow-greenish fragments of anglesite were found in sample #32 and identified by  $\mu$ Raman spectroscopy.

*Baryte*: a single vitreous and colorless crystal fragment of baryte, identified by SEM-EDS, was found in sample #32.

*Apatite*: crystals belonging to this group of minerals were not investigated in detail in order to better define their nature; they were just analyzed by SEM-EDS revealing the occurrence of Ca, P and F in the majority of studied crystals. Apatite commonly forms rounded grains and much more rarely clear crystals still showing many small faces.

*“Monazite”*: it was found within samples #4a, #21 and #32 and identified by SEM-EDS and XRPD. The few grains identified as “monazite” appear rounded in shape, somewhat “polished” and with a waxy lustre (Fig. 5d). They have a pale ochre-yellow color. In sample #32 we found a mica crystal covered by hundreds of tiny euhedral crystals of “monazite”.

### Silicates

*Almandine*: this garnet should be considered as one of the components of the siliciclastic rocks of the Monti Pisani. It occurs as reddish, rounded and abraded dodecahedral crystals; it was sporadically found in samples #5, #21, #29, #32 (Fig. 5f).

*Diopside-Hedenbergite*: pyroxenes were not fully characterized and they were identified through SEM-EDS and XRPD analyses. Found in samples #1, #7, #12, #16, #19, #32 (Fig. 6a).

*Epidote*: this quite common species was identified by SEM-EDS and XRPD analyses. The rounded and abraded crystal fragments still preserve the prismatic habitus and the olive-green color typical of this mineral.

*Kyanite*: three prismatic colorless crystals of kyanite were found in sample #32 (Fig. 6b).

*Sillimanite*: two grains of this mineral were found in sediments from Rio San Pantaleone (sample #29). One is a single, elongated, prismatic crystal. It is clear and colorless. The other grain is a greyish, fibrous, microcrystalline aggregate. For both grains the identification

was performed by XRPD using a Gandolfi camera. The identification of the second grain was confirmed by  $\mu$ Raman spectroscopy.

*Spessartine*: this garnet occurs as small clear fragments or euhedral crystals showing the typical orange color (samples #12, #32). The crystal of Fig. 6c shows the combination of dodecahedral and trapezohedral crystal faces. Spessartine was identified by SEM-EDS and XRPD.

*Staurolite*: this silicate was found in sample #32 both as euhedral prismatic crystals (Fig. 6d) or as intergrowths with kyanite. Staurolite was identified by  $\mu$ Raman spectroscopy.

*Tourmaline*: numerous glassy crystals, usually dark grape-marc-colored, were identified as tourmaline. Sometimes the crystals are strongly zoned, exhibiting a termination that can be either colorless or darker. Even if tourmaline occurs in many samples, it was found in abundance in samples #7, #14, #P24, #25, #32. Crystals show the elongated prismatic habitus typical of the species, with striated prism faces and rhombohedral sharp terminations. They do not show signs of abrasion (Fig. 6e). Small crystals of tourmaline were found in situ within quartz veins in various localities of the Monti Pisani (Orlandi, 1984); this observation, along with the well-preserved shape of the crystals, suggests that this mineral is another species of the Monti Pisani hydrothermal activity (Dini *et al.*, 1998). Many SEM-EDS analyses and a single EPM analysis, coupled with XRPD data indicate that these tourmalines could be related to the dravite end-member.

*Tremolite-actinolite*: based on SEM-EDS and XRPD analyses some elongated crystal fragments were ascribed to this series of amphiboles. These grains, found in sample #12, have a greyish color and a glassy lustre and show an abraded surface.

*Zircon*: owing to the hardness and inalterability of this mineral, most of the crystals, found abundantly in almost all samples, show well-preserved crystal shapes (Fig. 6f). Zircon occurs as more or less elongated prisms with well-developed bi-pyramidal faces. Most crystals are colorless, but pink crystals also occur. A lower number of zircon crystals have blunt edges and look abraded.

### Weird minerals (?) and other material

*Tin-mercury alloy*: the unique fragment of this species (sample #1) was identified by SEM-EDS and XRPD using a Gandolfi camera, and by comparison with a synthetic analogue. It occurs as a small, shapeless, opaque grain with sub-metallic lustre; the same fragment was analyzed by single crystal X-ray diffraction using a Weissenberg camera. These data allowed to assess that the grain was a single crystal and confirmed the cubic symmetry of the species.

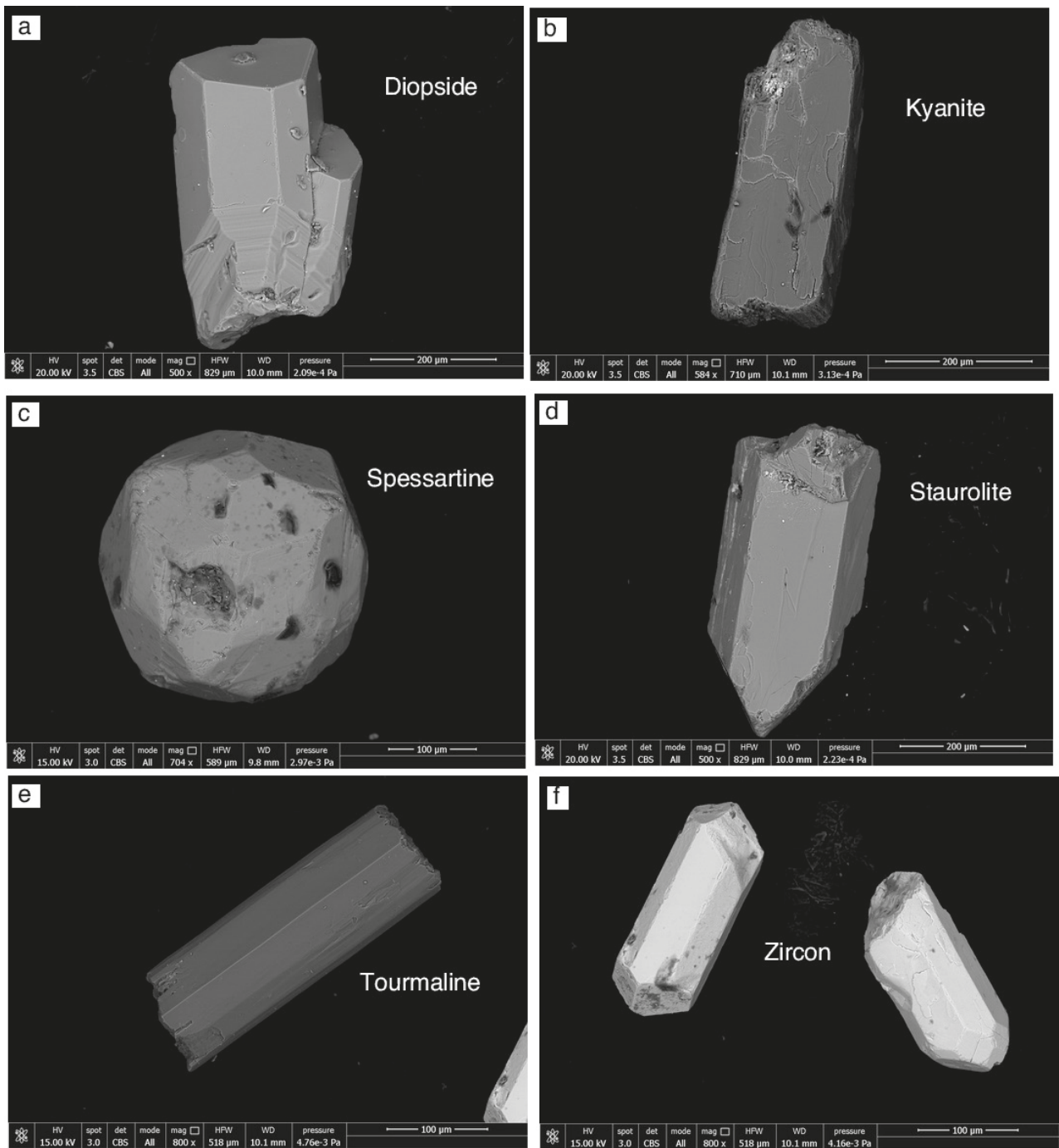


Figure 6. Back-scattered electron images of high-density crystals and crystal fragments extracted from sample #32 (Rio San Pantaleone, Santa Maria del Giudice, Lucca). a) two sharp, euhedral crystals of diopside; b) subhedral, abraded crystal of kyanite; c) euhedral, slightly abraded, dodecahedral + trapezohedral crystal of spessartine; d) euhedral prismatic crystal of staurolite; e) sharp, euhedral crystals of tourmaline; f) two euhedral, partially abraded crystal of zircon.

*Magnetic microspherules*: they are quite common in almost all the samples. The most abundant types are little, metallic, black spherules mostly made of magnetite (SEM-EDS and XRPD analyses). Magnetic microspherules were already found on the Monti Pisani and described by Cascella *et al.* (1995). The latter authors proposed an extraterrestrial origin for these spherules. Besides the opaque magnetic microspherules, we also found glassy transparent microspherules. They are colorless, yellow or greenish and amorphous under X-ray diffraction. This kind of material could be either natural and extraterrestrial or anthropogenic. Further, more specific analyses are needed to fully characterize these non-magnetic microspherules.

*Moissanite?*: the question mark points to the uncertain nature of the silicon carbide (SiC) crystals found in the stream sediments of Monti Pisani that could be either natural or anthropogenic. In the following description we will use the name of the mineral moissanite, hoping to ascertain its eventual natural origin with a more detailed study to come. Moissanite and carborundum (synthetic SiC) are indistinguishable with conventional chemical and XRD data. Their distinction requires more specific methods, such as the determination of the carbon isotope composition, the trace-element composition, or the study of the fluid and solid inclusions. Silicon carbide, both natural and synthetic, occurs in large number of polytypes (predominantly hexagonal or rhombohedral). Most of the natural moissanite grains are 6H and 15R polytypes (Shiryaev *et al.*, 2011). Moissanite has been found in Nature in many different occurrences (Trumbull *et al.*, 2009): the first finding and description is due to Henri Moissan (Moissan, 1904) who identified the mineral in the Canyon Diablo iron meteorite (Barringer Crater, Arizona); however, the natural origin of the mineral was long questioned as it was hypothesized that the meteorite had been cut using also carborundum (produced for the first time just two years before) as an abrasive. Other occurrences of natural moissanite are: kimberlite (Leung *et al.*, 1990; Shiryaev *et al.*, 2011), some unusual metasomatic rocks (Lyakhovich, 1980; Di Pierro *et al.*, 2003), peridotite and serpentinite (Xu *et al.*, 2008), and podiform chromite (Bai *et al.*, 2000).

Within our samples we found a total of 7 crystal fragments distributed in 4 different samples (#3, #4a, #16, #29). The mineral was identified by XRPD using a Gandolfi camera, and by SEM-EDS analyses. Moissanite occurs as transparent grains, few tens of  $\mu\text{m}$  large, showing the typical bright, metallic-blue color. Since the study of De Fonte (1996), the finding of this species was considered as due to a contamination of carborundum, a material widely used as abrasive due to its very high hardness. At present, we do not exclude the possibility of a natural origin of this mineral.

Indeed after successive sampling in the Monti Pisani area and in other locality of Tuscany, we found two more crystals of moissanite in Rio San Pantaleone and Botro della Fonte del Porco streams, whereas in about 40 new samples taken from other parts of Tuscany this mineral was never observed. The latter samples were collected in the beds of streams whose drainage basins do not contain the siliciclastic Paleozoic-Triassic rocks forming the Monti Pisani. On these bases we do not discard the hypothesis that the moissanite crystal fragments could be detrital minerals contained in the siliciclastic rocks of the Monti Pisani.

## CONCLUSIONS

The survey aimed at finding the primary source of the cinnabar crystals commonly found in the stream sediments from Monti Pisani, led to the discovery of a small area of low-temperature hydrothermal alteration. This area is localized at an altitude of 380 m a.m.s.l. about 1.5 km due south-east of the village of Vorno (Lucca). Crystalline cinnabar was found at a maximum concentration of about 110 mg/kg, suggesting that more important cinnabar occurrences could be found in the nearby area. These mineralizations are likely related to the hydrothermal events that originated the widespread system of quartz  $\pm$  siderite veins characterizing the meta-siliciclastic rocks of Monti Pisani (Dini *et al.*, 1998). A similar hydrothermal activity was possibly responsible for the cinnabar mineralization known since the XIX century (D'Achiardi, 1872-73) and hosted within the Jurassic carbonatic rocks of Monte delle Fate, close to the village of San Giuliano Terme (PI).

A by-product of this systematic survey was the finding of many high-density minerals that are primary clastic components of the meta-sedimentary rocks of the Monti Pisani. These rocks formed in a continental setting following the erosion of the Variscan Belt and were successively metamorphosed under greenschist facies conditions during the Alpine Orogeny. Among these minerals are worth-mentioning some spinels (e.g., gahnite), sillimanite, kyanite and corundum, besides more common species such as garnets, rutile, zircon, apatite, pyroxenes, staurolite, amphiboles, epidote and monazite-(Ce). Other recovered high-density minerals are sourced in syn- or post-Alpine hydrothermal mineralizations. Sulfides (pyrite, cinnabar, sphalerite, chalcopyrite) belong very likely to this group. The extremely rare native mercury droplets, and the unique Sn-Hg alloy, unless their occurrence is imputable to anthropogenic contamination, are to be considered hydrothermal minerals. Tourmaline, a widespread and abundant mineral in many investigated samples, is often characterized by well-developed crystals with

sharp edges. Thus, this mineral is one of the phases formed during the late stages of the metamorphism affecting the rocks of the Monti Pisani.

The finding of native gold in particles larger than about 100  $\mu\text{m}$  should be considered rather exceptional in Tuscany. Indeed certain occurrences of "visible" gold are limited to the Buca dell'Angina mine (Peloux, 1922), the Le Cetine di Cotorniano mine (Menchetti & Batoni, 2015), and the skarn outcrop of Punta del Fenaio (Giglio Island; Dini & Orlandi, 2010).

Lastly, the occasional discovery of fragments of SiC should be further investigated to ascertain its natural (moissanite) or anthropogenic (carborundum) origin. Indeed, the natural occurrences of this mineral are more common than thought few years ago. The determination of the carbon isotope composition of these crystals and the study of their possible solid inclusions are therefore mandatory to definitely establish the origin of this material.

#### ACKNOWLEDGEMENTS

The authors wish to thank Alberto Ghelardini for his help during sample collection and preparation, and Daniela Mauro for her assistance with  $\mu\text{Raman}$  analyses. Cristian Biagioni is greatly acknowledged for his critical review of the manuscript.

#### REFERENCES

- AICHLER J., MALEC J., VEČEŘA J., HANŽL P., BURIÁNEK D., SIDORINOVÁ T., TÁBORSKY Z., BOLORMAA K., BYAMBASUREN D., 2008. Prospection for gold and new occurrences of gold-bearing mineralization in the eastern Mongolian Altay. *Journal of Geosciences* 53: 123-138.
- BAI W., ROBINSON P.T., FANG Q., YANG J., YAN B., ZHANG Z., HU X.-F., ZHOU M.-F., MALPAS J., 2000. The PGE and base-metal alloys in the podiform chromitites of Luobusa ophiolite, southern Tibet. *Canadian Mineralogist* 38: 585-598.
- BIAGIONI C., 2009. Minerali della Provincia di Lucca. Ed. Associazione Micro-Mineralogica Italiana, Cremona.
- CASCELLA A., GINI C., GUELFI F., ORLANDI P., 1995. Sferule metalliche magnetiche nelle sabbie dei torrenti dei Monti Pisani. *Rivista Mineralogica Italiana* 1995-2: 165-168.
- D'ACHIARDI A., 1872-73. Mineralogia della Toscana. Tipografia Nistri, Pisa.
- DALL'AGLIO M., DA ROIT R., ORLANDI C., TONANI F., 1966. Prospezione geochimica del mercurio. Distribuzione del mercurio nelle alluvioni della Toscana. *L'Industria Mineraria* 17: 391-398.
- DE FONTE L., 1996. Il cinabro dei M.ti Pisani. Unpublished Thesis. Università di Pisa.
- DI PIERRO S., GNOS E., GROBETY B.H., ARMBRUSTER T., BERNASCONI S.M., ULMER P., 2003. Rock-forming moissanite (Natural  $\alpha$ -silicon carbide). *American Mineralogist* 88: 1817-1821.
- DINI A., ORLANDI P., 2010. A new gold-bismuth occurrence at Punta del Fenaio (Giglio Island, Tuscany). *Atti della Società Toscana di Scienze Naturali, Memorie, Serie A* 115: 73-82.
- DINI A., ORLANDI P., PROTANO G., RICCOBONO F., 1998. Le vene di quarzo del Complesso Metamorfico dei Monti Pisani (Toscana): caratterizzazione strutturale, mineralogia ed inclusioni fluide. *Atti della Società Toscana di Scienze Naturali, Memorie, Serie A* 105: 113-136.
- LEUNG I., GUO W., FRIEDMAN I., GLEASON, J., 1990. Natural occurrence of silicon carbide in a diamondiferous kimberlite from Fuxian. *Nature* 346: 352-354.
- LYAKHOVICH V.V., 1980. Origin of accessory moissanite. *International Geology Review* 22: 961-970.
- MENCHETTI S., BATONI M., 2015. Le Cetine di Cotorniano: miniere e minerali. Ed. Associazione Micro-Mineralogica Italiana, Cremona.
- MOISSAN H., 1904. Nouvelles recherches sur la météorite de Cañon Diablo. *Comptes Rendus* 139: 773-786.
- ORLANDI P., 1984. Segnalazione di nuove specie mineralogiche da località italiane. *Rivista Mineralogica Italiana* 2/1984, 33-40.
- PELLOUX A., 1922. La zona metallifera del Bottino e della Valle di Castello. I suoi minerali e le sue miniere. *Memorie della Accademia Lunigianese di Scienze* 3: 39-83.
- RAU A., TONGIORGI M., 1974. Geologia dei Monti Pisane a SE della Valle del Guappero. *Memorie della Società Geologica Italiana* 13: 227-408.
- SHIRYAEV A.A., GRIFFIN W.L., STOYANOV E., 2011. Moissanite (SiC) from kimberlites: polytypes, trace elements, inclusions and speculations on origin. *Lithos* 122: 152-164.
- TRUMBULL R.B., YANG J.-S., ROBINSON P.T., DI PIERRO S., VENNE-MANN T., WIEDENBECK M., 2009. The carbon isotope composition of natural SiC (moissanite) from the Earth's mantle: new discoveries from ophiolites. *Lithos* 113: 612-620.
- XU S., WU W., XIAO W., YANG J., CHEN J., YI S., LIU Y., 2008. Moissanite in serpentinite from the Dabie Mountains in China. *Mineralogical Magazine* 72: 899-908.

(ms. pres. 30 agosto 2019; ult. bozze 1 ottobre 2019)

Edizioni ETS

Palazzo Roncioni - Lungarno Mediceo, 16, I-56127 Pisa

[info@edizioniets.com](mailto:info@edizioniets.com) - [www.edizioniets.com](http://www.edizioniets.com)

Finito di stampare nel mese di dicembre 2019